

Experimental determination of the Weiss temperature of Mn₁₂-ac and Mn₁₂-ac-MeOH

Shiqi Li, Lin Bo, Bo Wen, and M. P. Sarachik

Department of Physics, City College of New York, CUNY, New York, New York 10031, USA

P. Subedi and A. D. Kent

Department of Physics, New York University, New York, New York 10003, USA

Y. Yeshurun

*Department of Physics, City College of New York, CUNY, New York, New York 10031, USA;**Department of Physics, New York University, New York, New York 10003, USA;**and Department of Physics, Institute of Nanotechnology, Bar-Ilan University, Ramat-Gan 52900, Israel*

A. J. Millis

Department of Physics, Columbia University, New York, New York 10027, USA

C. Lampropoulos, S. Mukherjee, and G. Christou

Department of Chemistry, University of Florida, Gainesville, Florida 32611, USA

(Received 19 August 2010; published 3 November 2010)

We report measurements of the susceptibility in the temperature range from 3.5 to 6.0 K of a series of Mn₁₂-ac and Mn₁₂-ac-MeOH samples in the shape of rectangular prisms of length l_c and square cross section of side l_a . The susceptibility obeys a Curie-Weiss law, $\chi=C/(T-\theta)$, where θ varies systematically with sample aspect ratio. Using published demagnetization factors, we obtain θ for an infinitely long sample corresponding to intrinsic ordering temperatures $T_c \approx 0.85$ K and ≈ 0.74 K for Mn₁₂-ac and Mn₁₂-ac-MeOH, respectively. The difference in T_c for two materials that have nearly identical unit cell volumes and lattice constant ratios suggests that, in addition to dipolar interactions, there is a nondipolar (exchange) contribution to the Weiss temperature that differs in the two materials because of the difference in ligand molecules.

DOI: [10.1103/PhysRevB.82.174405](https://doi.org/10.1103/PhysRevB.82.174405)

PACS number(s): 75.50.Xx, 75.30.Et, 75.30.Cr

I. INTRODUCTION

The magnetic susceptibility, χ , is given within the mean-field approximation by the Curie-Weiss law, $\chi=C/(T-T_c)$, where C is a material-specific Curie constant, T is the absolute temperature, and the Weiss temperature T_c is the (approximate) temperature below which the system is ferromagnetic or antiferromagnetic, depending on the sign of T_c . In order to determine the susceptibility and T_c experimentally, however, the measured values need to be corrected to account for a demagnetizing field, H_d , which depends on sample geometry, as well as the value of the susceptibility itself.

In this paper we report measurements of the magnetization and susceptibility of a series of samples of two different variants of the molecular magnet Mn₁₂-ac: the usual, much-studied form referred to as Mn₁₂-ac and a new form abbreviated as Mn₁₂-ac-MeOH. The measurements were taken for a series of samples in the shape of rectangular prisms with approximately square cross section l_a^2 and length l_c . The susceptibility is found to obey the expected Curie-Weiss form, $\chi=C/(T-\theta)$,^{1,2} but with a Curie-Weiss θ that varies systematically with the sample aspect ratio l_c/l_a . Using demagnetization factors calculated by Chen, Pardo, and Sanchez,^{3,4} we have deduced the value of θ for an infinitely long sample, corresponding to the intrinsic ordering temperature T_c for the two materials.

II. EXPERIMENTAL PROCEDURE

Parallel studies were carried out on single crystals of the usual form of Mn₁₂-ac, [Mn₁₂O₁₂(O₂CMe)₁₆(H₂O)₄]·2MeCO₂H·4H₂O, and a new recently synthesized form Mn₁₂-ac-MeOH, [Mn₁₂O₁₂(O₂CMe)₁₆(MeOH)₄]·MeOH. The normal form [space group $I\bar{4}$; unit-cell parameters $a=b=17.1668(3)$ Å, $c=12.2545(3)$ Å, $Z=2$, and $V=3611.39$ Å³ at 83 K] (Ref. 5) and the new form [space group $I\bar{4}$; unit-cell parameters $a=b=17.3500(18)$ Å, $c=11.9971(17)$ Å, $Z=2$, and $V=3611.4$ Å³ at -100 °C] (Ref. 6) of Mn₁₂-ac are quite similar but they differ in the solvent molecules of crystallization that lie in between the Mn₁₂ molecules. In normal Mn₁₂-ac, each Mn₁₂ molecule forms O-H···O hydrogen bonds with n ($n=0-4$) of the surrounding MeCO₂H molecules while in Mn₁₂-ac-MeOH, the lattice MeOH molecules form no hydrogen bonds to the Mn₁₂ molecules.

Sample preparations for Mn₁₂-ac and Mn₁₂-ac-MeOH are described in Refs. 7 and 6, respectively. The samples were in the form of rectangular prisms of dimensions $l_a \times l_b \times l_c$ ($l_a \approx l_b$) with l_a varying from ~ 0.1 to ~ 0.4 mm. The dimensions of the samples were measured under a microscope by a small scaler. Data were taken for aspect ratios (l_c/l_a) varying from 0.75 to 9.57 for Mn₁₂-ac, and from 1.45 to 4.9 for Mn₁₂-ac-MeOH. The range of aspect ratios was determined by sample availability.

The magnetization was measured in a commercial Quantum Design magnetic property measurement system

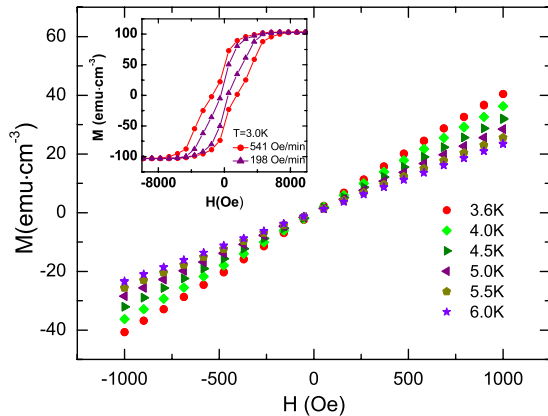


FIG. 1. (Color online) Magnetization of $\text{Mn}_{12}\text{-ac}$ as a function of longitudinal magnetic field for different temperatures above the blocking temperature T_B . Sufficiently slow sweep rates are chosen to ensure that the system is in equilibrium. Inset: open hysteresis loops displaying the familiar steps associated with spin tunneling in molecular magnets are obtained at lower temperature and higher sweep rates.

(MPMS) superconducting quantum interference device (SQUID)-based magnetometer. The crystals were mounted using a minimum amount of Dow Corning high vacuum grease. As the $\text{Mn}_{12}\text{-ac-MeOH}$ crystals are known to degrade rapidly when removed from their mother liquor, care was taken to quickly transfer these samples into paraffin oil using a paraffin-coated stick. Hysteresis curves taken below the blocking temperature displayed the steps characteristic of tunneling in single molecule magnets, indicating the samples had not degraded significantly during handling. Care was taken to align the c axis of the crystals parallel to the magnetic field.

The measured magnetization should be normalized by the volume (or mass) of each sample. In our case, the samples are so small that neither the volume, V , nor the mass, m ($\approx 10^{-5}$ g), can be measured accurately. The SQUID-based magnetometer, however, provides a precise measure of the saturation magnetization, which is proportional to the volume. We therefore normalized the data for each sample by M_{sat} and, noting that there are two Mn_{12} molecules, each with spin $S=10$ in a (body-centered-cubic) unit cell of known volume, we applied a (calculated) conversion factor $M_{sat}=2gS\mu_B/V_{cell}=102.7$ emu/cm³ to obtain the magnetization and the susceptibility in cgs units.

$\text{Mn}_{12}\text{-ac}$ molecules behave as nanomagnets with spin $S=10$ in crystals with strong uniaxial magnetic anisotropy along the c axis of the crystals. Modeled as a double-well potential, slow relaxation below a sweep-rate-dependent blocking temperature T_B gives rise to hysteresis in M versus H , as shown in the inset of Fig. 1; the stepwise change in magnetization is typical for molecular magnets, where steps occur due to spin tunneling at values of longitudinal magnetic field where energy levels corresponding to different spin projections cross on opposite sides of the anisotropy barrier. Equilibrium measurements from which the susceptibility can be obtained therefore require sufficiently high temperatures (above blocking) and/or slow sweep rates. Revers-

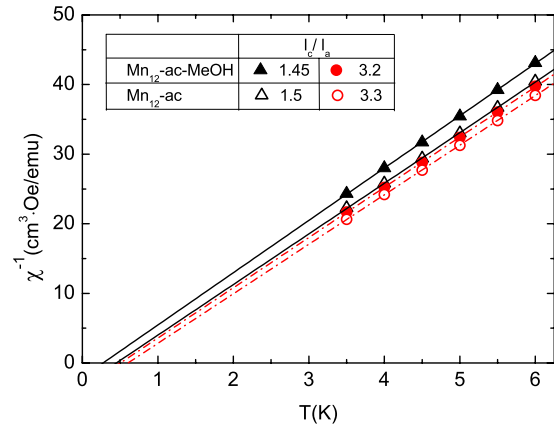


FIG. 2. (Color online) The inverse susceptibility of $\text{Mn}_{12}\text{-ac}$ as a function of temperature for two samples each of $\text{Mn}_{12}\text{-ac}$ and $\text{Mn}_{12}\text{-ac-MeOH}$ with different (matched) aspect ratios, as indicated. The dotted-dashed and solid lines are for aspect ratios ≈ 3.3 and ≈ 1.5 , respectively. Extension of the straight lines yield temperature intercepts, θ , that vary with aspect ratio and are different for the two materials.

ible behavior, signaling equilibrium, was obtained in our experiments above a blocking temperature on the order of 3–4 K for the sweep rates used. As a consequence, our susceptibility measurements were limited to temperatures above 3 K.

III. EXPERIMENTAL RESULTS

As shown in Fig. 1, data for the magnetization M versus H were obtained in the linear regime. The susceptibility given by the slope of these straight lines, $\chi=dM/dH|_{H=0}$, increases with decreasing temperature, as expected.

Figure 2 shows the inverse of the susceptibility as a function of temperature for two crystals of $\text{Mn}_{12}\text{-ac}$ with aspect ratios $l_c/l_a=1.5$ and 3.3 , and two samples of $\text{Mn}_{12}\text{-ac-MeOH}$ with aspect ratios closely matched to those of $\text{Mn}_{12}\text{-ac}$. The straight lines demonstrate that the susceptibility obeys a Curie-Weiss law, $\chi=C/(T-\theta)$. The lines are approximately parallel, indicating that the Curie constant, $C=0.138$ for the two systems is approximately the same, as expected. For each material, ($\text{Mn}_{12}\text{-ac}$ or $\text{Mn}_{12}\text{-ac-MeOH}$), the intercept θ is larger for the larger aspect ratio. A cross comparison reveals that for the same aspect ratio, the intercept is smaller for $\text{Mn}_{12}\text{-ac-MeOH}$ than it is in $\text{Mn}_{12}\text{-ac}$.

The intercept θ is shown in Fig. 3 as a function of aspect ratio for $\text{Mn}_{12}\text{-ac}$ and $\text{Mn}_{12}\text{-ac-MeOH}$. For each material, θ increases with increasing aspect ratio, asymptotically approaching a limiting value as the sample becomes longer and/or thinner. While the behavior as a function of aspect ratio is qualitatively similar for the two materials, it is clear that θ is smaller in $\text{Mn}_{12}\text{-ac-MeOH}$ than in $\text{Mn}_{12}\text{-ac}$ for every aspect ratio over the entire range of our measurements.

IV. THEORETICAL ANALYSIS

The study of demagnetization factors of homogeneous bodies has been a classical topic in magnetism.^{8,9} Demagne-

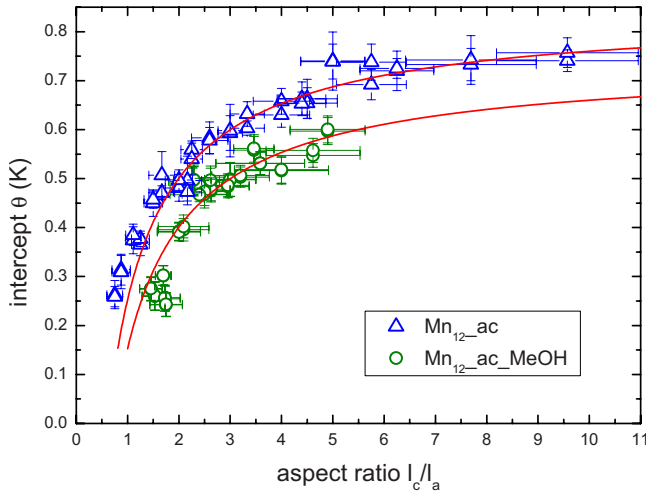


FIG. 3. (Color online) Temperature intercept θ as a function of aspect ratio for $\text{Mn}_{12}\text{-ac}$ (triangles) and $\text{Mn}_{12}\text{-ac-MeOH}$ (circles). The lines denote fits obtained as described in the text.

tization factors have been calculated for many different shapes, including ellipsoids and spheres, rods and disks, and rectangular prisms.^{3,4,9,10} In the analysis described below, we use published tables of the demagnetization factors for bars with square cross section^{3,4} to fit the data of Fig. 3 and determine the limiting value of $\theta_{CW}=T_c$ for very large aspect ratio.

The magnetic susceptibility measured in our experiment, $\chi=M/H_{ext}$, is deduced from the slope of the straight lines of M versus the externally applied magnetic field H_{ext} shown in Fig. 1. To obtain the true susceptibility, $\chi=M/H_{tot}$, one needs to use the total magnetic field, $H_{tot}=H_{ext}+H_d$, where H_d is the demagnetizing field. The demagnetizing field is opposite to and proportional to the magnetization of the sample, $H_d=-N_dM$, where N_d depends primarily on the geometry of the sample and, to a lesser degree, the susceptibility of the material (see Chen *et al.*⁹ and references therein). Except for ellipsoidal specimens, the demagnetization factor varies from point to point and one needs to apply an averaged demagnetization factor that depends on the type of measurement, e.g., a measurement taken by a coil wound around the middle or a measurement of the entire sample. For our SQUID-based measurements of small samples, the appropriate factor is the ratio of the average demagnetizing field to the average magnetization of the entire sample, the so-called magnetometric demagnetization factor N_m .

The magnetometric demagnetization factor, N_m , was obtained for the aspect ratios of our crystals by interpolation using the published tables for bars of square cross section.^{3,4} We select the values listed for $\chi=0$ since the small susceptibility of our samples produces demagnetizing fields that are small compared to the applied magnetic field. The resulting curve for N_m versus aspect ratio is shown in the inset of Fig. 4. Combining this with the information in Fig. 3, one obtains θ versus N_m shown in the main part of the figure for Mn_{12} and $\text{Mn}_{12}\text{-ac-MeOH}$.

The simplest mean-field derivation of the Curie-Weiss law incorporates the effect of interactions by postulating a “molecular field,” H_m . The demagnetizing field H_d can be intro-

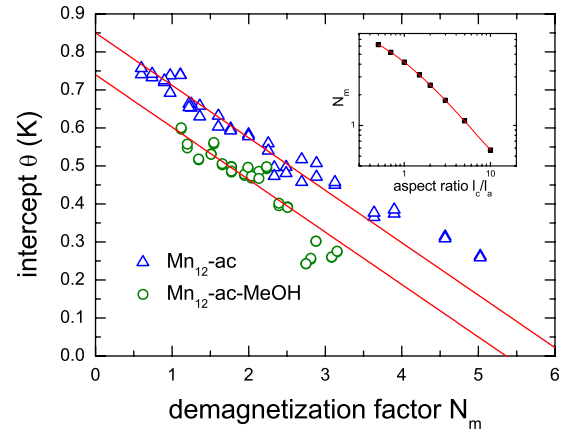


FIG. 4. (Color online) Temperature intercept θ as a function of demagnetization factor N_m (in cgs units) for $\text{Mn}_{12}\text{-ac}$ (triangles) and $\text{Mn}_{12}\text{-ac-MeOH}$ (circles). Approximate fits are denoted by the solid lines with (negative) slopes constrained to be equal to the Curie constant $C=0.138$ [see Eq. (1)]. Inset: magnetometric demagnetization factor N_m as a function of aspect ratio; values of N_m are obtained by interpolation from the tables published by Chen, Pardo and Sanchez (Refs. 3 and 4).

duced in a similar way by writing $H_{tot}=H_{ext}+H_m+H_d$, from which one obtains

$$\theta = \theta_{CW} \left(\frac{c}{a} \right) - CN_m \left(\frac{l_c}{l_a} \right), \quad (1)$$

where C is the Curie constant. The first term in this expression depends only on lattice properties such as c/a and the local chemistry (the molecule solvent and ligand structure) and is independent of the aspect ratio while the second term depends only on the shape of the crystal and vanishes in the limit of infinite aspect ratio l_c/l_a . For a particular material, say, $\text{Mn}_{12}\text{-ac}$, the lattice properties such as c/a and local chemistry are the same for all samples with different aspect ratios, and the value of θ_{CW} in Eq. (1) can be interpreted empirically as the intrinsic Curie-Weiss temperature T_c obtained in the limit of infinite aspect ratio.¹¹

As shown in Fig. 4, θ depends linearly on N_m , as expected from Eq. (1), for both $\text{Mn}_{12}\text{-ac}$ and $\text{Mn}_{12}\text{-ac-MeOH}$. Guided by Eq. (1), the slopes of the solid lines drawn in the figure were constrained to the value $C=0.138$ obtained from the data of Fig. 2, yielding $\theta_{CW}=T_c \approx 0.85$ K for $\text{Mn}_{12}\text{-ac}$ and $T_c \approx 0.74$ K for $\text{Mn}_{12}\text{-ac-MeOH}$.

Theoretical calculations^{13–15} have been carried out for $\text{Mn}_{12}\text{-ac}$ based on models that consider dipolar interactions only, on the assumption that other terms (for example, direct exchange from overlap of wave functions) can be neglected. Chudnovsky and Garanin¹³ predicted ferromagnetic ordering of elongated crystals of $\text{Mn}_{12}\text{-ac}$ below 0.8 K; Garanin’s¹⁴ recent investigation of elongated box-shape crystals yielded an ordering temperature ~ 0.71 K. Values of $J(c/a)=\theta_{CW}$ can also be obtained from the work of Millis *et al.*,¹⁵ who write the susceptibility as

$$\frac{1}{\chi} = \frac{T - \theta_{CW}}{C} = \frac{T - 2E_{dip}J}{C}, \quad J = J_{SR} + 4\pi/3. \quad (2)$$

Here E_{dip} is the dipolar interaction and the short-range contribution J_{SR} , depends on the details of the crystal structure. For Mn_{12} -ac, with lattice constants $a=b=17.1668(3)$ Å, $c=12.2545(3)$ Å, one obtains $J \approx 5.287$ while for Mn_{12} -ac-MeOH with $a=b=17.3500(18)$ Å, $c=11.9971(17)$ Å, and $J \approx 5.514$.¹² The strength of the dipolar interaction, $E_{dip} \approx 0.078$ K, is essentially the same for the two materials as their unit cells have the same volume within 0.01%. This yields $\theta_{CW} \approx 0.82$ K for Mn_{12} -ac and ≈ 0.86 K for Mn_{12} -ac-MeOH.

The crystal structures of Mn_{12} -ac-MeOH and Mn_{12} -ac are quite similar: the unit-cell parameters and unit volumes cell are nearly identical, and the strength of the dipolar interactions are expected to be essentially the same. These similarities are reflected by the nearly identical Curie constants obtained experimentally for the two systems. By contrast, however, the values of the Curie-Weiss θ_{CW} 's are clearly and consistently smaller for Mn_{12} -ac-MeOH than they are in Mn_{12} -ac, as shown in Figs. 3 and 4, implying that the magnetic interactions are weaker in Mn_{12} -ac-MeOH. We note that although the unit-cell parameters are nearly identical, the two systems have different ligands bridging the Mn_{12} molecules. A possible explanation for the different interaction strengths in the two materials may be that, in addition to the dipolar interactions, quantum-mechanical exchange deriving from wave function overlap plays a significant role. In particular, our results suggest that there is an extra direct ex-

change contribution of antiferromagnetic sign in Mn_{12} -ac-MeOH.

V. SUMMARY

The susceptibility of Mn_{12} -ac and Mn_{12} -ac-MeOH has been measured for a series of samples in the shape of rectangular prisms of length l_c and square cross section of side l_a . Fits to a Curie-Weiss law, $\chi = C/(T - \theta)$, yield values for θ that vary systematically with the aspect ratio, l_c/l_a . Using published values of the demagnetization factor^{3,4} we have deduced values of $\theta_{CW} = T_c$ that are surprisingly different for Mn_{12} -ac and Mn_{12} -ac-MeOH, two materials that have nearly identical crystal structures but different ligands bridging the Mn_{12} molecules in the crystal. This suggests that, in addition to dipolar interactions, there is a nondipolar (exchange) contribution to the Weiss temperature that is different for the different ligand molecules in the crystal.

ACKNOWLEDGMENTS

We thank Dimitar Dimitrov for valuable technical help during the initial phases of the experiment. We acknowledge illuminating discussions with D. M. Garanin, E. M. Chudnovsky, and J. R. Friedman. Support for G.C. was provided by NSF under Grant No. CHE-0910472; A.D.K. acknowledges support by NSF under Grant No. DMR-0506946 and ARO under Grant No. W911NF-08-1-0364; A.J.M. acknowledges support of NSF under Grant No. DMR-0705847; M.P.S. acknowledges support from NSF under Grant No. DMR-0451605; Y.Y. acknowledges support of the Deutsche Forschungsgemeinschaft through a Deutsch-Israelische Projektkooperation (DIP).

¹F. Luis, J. Campo, J. Gomez, G. J. McIntyre, J. Luzon, and D. Ruiz-Molina, *Phys. Rev. Lett.* **95**, 227202 (2005).

²Bo Wen, P. Subedi, Lin Bo, Y. Yeshurun, M. P. Sarachik, A. D. Kent, A. J. Millis, C. Lampropoulos, and G. Christou, *Phys. Rev. B* **82**, 014406 (2010).

³E. Pardo, D.-X. Chen, and A. Sanchez, *IEEE Trans. Magn.* **40**, 1491 (2004).

⁴D.-X. Chen, E. Pardo, and A. Sanchez, *IEEE Trans. Magn.* **41**, 2077 (2005).

⁵A. Cornia, A. C. Fabretti, R. Sessoli, L. Sorace, D. Gatteschi, A.-L. Barra, C. Daiguebonne, and T. Roisnel, *Acta Crystallogr., Sect. C: Cryst. Struct. Commun.* **58**, m371 (2002).

⁶G. Redler, C. Lampropoulos, S. Datta, C. Koo, T. C. Stamatatos, N. E. Chakov, G. Christou, and S. Hill, *Phys. Rev. B* **80**, 094408 (2009).

⁷T. Lis, *Acta Crystallogr., Sect. B: Struct. Crystallogr. Cryst. Chem.* **36**, 2042 (1980).

⁸B. D. Cullity and C. D. Graham, *Introduction to Magnetic Materials*, 2nd ed. (Wiley, Hoboken, NJ, 2009).

⁹D.-X. Chen, J. A. Brug, and R. B. Goldfarb, *IEEE Trans. Magn.*

27, 3601 (1991).

¹⁰D.-X. Chen, E. Pardo, and A. Sanchez, *J. Magn. Magn. Mater.* **306**, 135 (2006).

¹¹Samples of widely different size with the same aspect ratio yielded closely similar results, confirming the validity of our analysis.

¹²Crystal structures have not been systematically measured as a function of temperature. In the absence of a change in phase, the lattice parameters are found to be about 1% smaller at 100 K than at room temperature, and the relative difference in c/a is expected to be much lower; we therefore assume that c/a is a constant.

¹³D. A. Garanin and E. M. Chudnovsky, *Phys. Rev. B* **78**, 174425 (2008).

¹⁴D. A. Garanin, *Phys. Rev. B* **81**, 220408 (2010); note that Garanin claims in this paper that finding the ordering temperature by linearly extrapolating the inverse susceptibility curve above the transition temperature does not provide a correct T_c .

¹⁵A. J. Millis, A. D. Kent, M. P. Sarachik, and Y. Yeshurun, *Phys. Rev. B* **81**, 024423 (2010).